Elsevier Editorial System(tm) for
International Journal of Pharmaceutics or its open access mirror
Manuscript Draft

Manuscript Number: IJP-D-19-01256R2

Title: Making Tablets for Delivery of Poorly Soluble Drugs Using Photoinitiated 3D Inkjet Printing

Article Type: Research Paper

Section/Category: Personalised Medicine

Keywords: delivery of a poorly soluble drug;
tablet;
additive manufacturing;
inkjet 3D printing;
UV photopolymerization;
personalized medicine;
carvedilol

Corresponding Author: Dr. Elizabeth A Clark, Ph.D.

Corresponding Author's Institution: University of Nottingham, University Park

First Author: Elizabeth A Clark, Ph.D.

Order of Authors: Elizabeth A Clark, Ph.D.; Morgan R Alexander, Ph.D.; Derek J Irvine, Ph.D.; Clive J Roberts, Ph.D.; Martin J Wallace; Jae X Yoo, Ph.D.; Ricky D Wildman, Ph.D.

Abstract: In this study, we investigate the viability of three-dimensional (3D) inkjet printing with UV curing to produce solid dosage forms containing a known poorly soluble drug, carvedilol. The formulation consists of 10 wt% carvedilol, Irgacure 2959, and a photocurable N-vinyl-2-pyrrolidone (NVP) and poly(ethylene glycol) diacrylate matrix, with the intention of forming an amorphous solid solution for release of carvedilol. Characterization of the printed tablets showed that the drug is an amorphous state and indicated hydrogen bonding interactions between the drug and cross-linked matrix. Several simple geometries (ring, mesh, cylinder, thin film) were printed, and the surface area to volume ratio of the prints was estimated. Over 80% carvedilol release was observed for all printed tablet geometries within ten hours. The release behaviour of carvedilol was fastest for the thin films, followed by the ring and mesh geometries, and slowest in the cylindrical forms. More rapid release was correlated to an increased surface area to volume ratio. This is the first study to implement 3D UV inkjet to make solid dispersion tablets suitable for poorly soluble drugs. Results also demonstrate that high drug-loaded tablets with a variety of release profiles can successfully be accessed with the same UV-curable inkjet formulation by varying the tablet geometry.

*Graphical Abstract (for review)

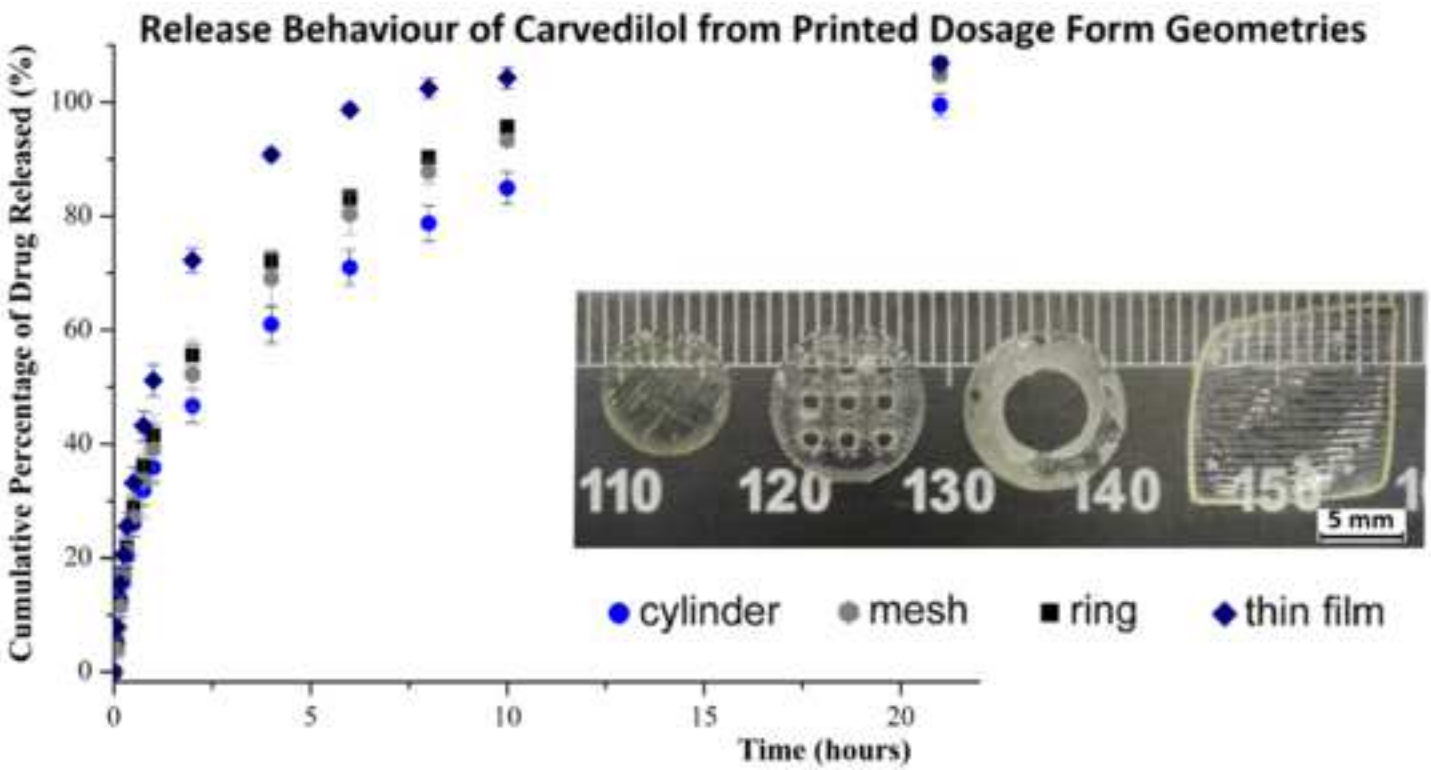

Making Tablets for Delivery of Poorly Soluble Drugs Using Photoinitiated 3D Inkjet Printing

Elizabeth A. Clark[a], Morgan R. Alexander[a], Derek J. Irvine[b], Clive J. Roberts[a], Martin J. Wallace[c], Jae Yoo[d], Ricky D. Wildman[b]*

[a] Advanced Materials and Healthcare Technologies, School of Pharmacy, The University of Nottingham, University Park, Nottingham, NG7 2RD, UK

[b] Centre for Additive Manufacturing, Advanced Manufacturing Building, The University of Nottingham, Jubilee Campus, Nottingham, NG8 1BB, UK

[c] Advanced Manufacturing Technology, GlaxoSmithKline (Ireland), 12 Riverwalk, Citywest, Business Campus, Dublin, 24, Ireland

[d] Advanced Manufacturing Technology, GlaxoSmithKline, 709 Swedeland Rd., UW2108, King of Prussia, PA 19406-0939, USA

[*] Corresponding author

E-mail: Ricky.Wildman@nottingham.ac.uk and Elizabeth.Clark@nottingham.ac.uk

Telephone: + 44 (0) 115 8466893

Centre for Additive Manufacturing, Advanced Manufacturing Building, The University of Nottingham, Jubilee Campus, Nottingham, NG8 1BB, UK

Abstract

In this study, we investigate the viability of three-dimensional (3D) inkjet printing with UV curing to produce solid dosage forms containing a known poorly soluble drug, carvedilol. The formulation consists of 10 wt% carvedilol, Irgacure 2959, and a photocurable N-vinyl-2-pyrrolidone (NVP) and poly(ethylene glycol) diacrylate matrix, with the intention of forming an amorphous solid solution for release of carvedilol. Characterization of the printed tablets showed that the drug is an amorphous state and indicated hydrogen bonding interactions between the drug and cross-linked matrix. Several simple geometries (ring, mesh, cylinder, thin film) were printed, and the surface area to volume ratio of the prints was estimated. Over 80% carvedilol release was observed for all printed tablet geometries within ten hours. The release behaviour of carvedilol was fastest for the thin films, followed by the ring and mesh geometries, and slowest in the cylindrical forms. More rapid release was correlated to an

increased surface area to volume ratio. This is the first study to implement 3D UV inkjet to make solid dispersion tablets suitable for poorly soluble drugs. Results also demonstrate that high drug-loaded tablets with a variety of release profiles can successfully be accessed with the same UV-curable inkjet formulation by varying the tablet geometry.

1. Introduction

Three-dimensional (3D) printing has been investigated as a novel route to manufacture tablets and has been shown to offer several potential benefits when compared to conventional processing methods. The FDA's approval of Spritam, the first binder inkjet 3D printed tablet [FDA, 2015], highlighted this approach as a viable manufacturing platform to produce highly porous tablets which exhibit novel rapid drug release. 3D printing, particularly fusion deposition modelling (FDM), paste extrusion and inkjet methods, have been reported to offer manufacturing routes that enable tablet personalization through multi-active delivery [Khaled et al., 2015; Khaled et al., 2014; Genina et al., 2017; Goyanes et al., 2015b]. These techniques have also demonstrated precise control over tablet geometry and porosity, which can impart tuneable control over drug dissolution [Kyobula et al., 2017; Goyanes et al., 2015; Rowe et al., 2000; Solanki et al., 2018; Chai et al., 2017; Yang et al., 2018].

3D inkjet printing is a non-contact, drop on demand printing process that has recently been investigated as a manufacturing process to produce solid oral dosage forms [Kyobula et al., 2017; Clark et al., 2017]. Kyobula et al. used hot melt 3D inkjet to produce complex geometries whereby the freezing of the printed ink was the solidification process being exploited. They demonstrated with this approach how tablet geometry and infill density could be adjusted to predictably tune the release of fenofibrate, a poorly soluble drug, from a beeswax matrix. Bioresorbable photocurable polymers have more recently been evaluated

for inkjet printing using high throughput screening. Selected UV inkjet printable paroxetine HCl loaded formulations were printed into films which exhibit long-term controlled release suitable for implant applications [Louzao et al., 2018]. Drug release behaviour of paclitaxel from solvent inkjet printed micro particle geometries has also been investigated with solvent inkjet for PLGA/dimethylacetamide formulations. Drug release was shown to rely on the ratio of surface area to print volume (SA/V) of the dosage forms [Lee et al., 2012]; this dependence has been described for FDM and SLA printed formulations [Goyanes et al., 2015; Martinez et al., 2018]. Acosta-Vélez et al. have researched inkjet dispensing to deposit photocurable ink into preformed tablet reservoirs to produce dosage forms for highly water soluble drugs [Acosta-Vélez et al., 2017]. Such photocurable resin formulations have been demonstrated for VAT polymerization printing of paracetamol, 4-Aminosalicylic acid [Wang 2016] acetylsalicylic acid [Vehse et al., 2014] and ibuprofen [Martinez et al., 2017]. More recently, liquid dispensing has also been combined with FDM printing to produce liquid capsules with immediate and extended release profiles for poorly soluble drugs [Okwuosa et al., 2018].

Carvedilol is a beta-blocker used to treat hypertension and heart failure [GSK, 2017]. It is nearly insoluble in water and simulated gastric fluid at pH 1.1. At pH values in the pharmaceutically relevant range of 1–8, the solubility of carvedilol in aqueous media ranges from about 0.01 to 1 mg/mL [Beattie et al., 2013]. The dissolution of carvedilol in acid medium is related to its ability to form protonated molecules [Beattie et al., 2013; Prado et al. 2014]. Formulation enhancement of the solubility of carvedilol in water at 27 °C has been documented for carvedilol: para sulphonato calixarene inclusion complexes [Menon et al., 2012; Beattie et al., 2013].

Carvedilol is commercially available in a range of low dose immediate and sustained release doses ranging from 3.125 mg to 80 mg [GSK, 2017]. These formulations use the relatively

poorly soluble crystalline sold state forms of carvedilol [Prado et al. 2014]. As a strategy to improve the bioavailability for poorly soluble APIs the use of soluble matrix materials, such as poly(N-vinyl-2-pyrrolidone) (PVP), [Singh et al., 2017; Patterson et al., 2007; Bley et al., 2010]], and poly(ethylene glycol) (PEG) [Bley et al., 2010; Chokshi et al., 2007; Singh et al., 2017; Yuvaraja and Khanam, 2014] are well established pharmaceutical excipients [Singh et al., 2017, Kalepu and Mekkanti, 2015]. Photocurable analogues of PEG and PVP have also been previously investigated with 3D printing. In particular, fabrication of biomedical devices with PEG(meth)acrylate macromers have been utilized in VAT polymerization, 3D inkjet, and multiphoton polymerization printing processes [Nguyen et al., 2013; Wang et al., 2016; Chan et al., 2010; Vehse et al., 2014; Ligon et al., 2017; Gu, et al., 2016; Seck et al., 2010; Dhariwala et al., 2004; Gao et al., 2015; Jansen et al., 2009; Gao et al., 2015; Guvendiren et al., 2017; Clark et al., 2017; Do et al., 2018]. N-vinyl-2-pyrrolidone (NVP), the monomeric precursor to polymeric PVP, can be incorporated as a reactive diluent into UV inkjet formulations, and is capable of copolymerizing with PEG diacrylate [Lee et al., 2013]. Incorporation of NVP into copolymer networks has been shown to enhance hydrophilicity [Korsmeyer and Peppas, 1984; Caló and Khutoryanskiy, 2015; Jansen et al., 2009] in medical devices such as HEMA-co-NVP contact lenses, and NVP has been reported to solubilize a variety of both soluble and poorly soluble APIs [Hacker et al., 2009; Knopp et al., 2015]. Accelerated photocuring speeds have been reported for NVP systems, including for 3D printed PDLLA 3-FAME/NVP resins [Jansen et al., 2009], [Hacker et al., 2009] and acrylate-co-NVP resins [White et al., 2006, Ergenc and Kizilel, 2011].

In our previous work we have applied inkjet with UV initiated curing as a route to 3D print tablets with controlled release of ropinirole HCl, a highly water soluble drug [Clark et al., 2017]. In this study, our goal is to formulate, print and characterize a solvent-free, UV ink for 3D inkjet printing a poorly soluble drug. The release behaviour, as well as the physical

properties of several printed solid dosage form geometries is therefore evaluated and compared to United States Pharmacopeia (USP) specifications.

2. Materials and methods

2.1. Materials

Irgacure 2959 (98%) was purchased from (BASF). Carvedilol (≥ 98.5%) was purchased from Carbosynth. Poly(ethylene glycol) diacrylate (number average molecular weight, M_n = 250 g/mol) and N-vinyl-2-pyrrolidone (> 99%) were purchased from Sigma-Aldrich. All materials were used as received.

2.2. Characterization of solid dosage dimensions

The dimensions of the printed dosages were measured with an electronic caliper (Products Engineering Corp.).

2.3. X-ray micro computed tomography (μCT) scanning

μCT scanning of the dosage forms was carried out on a Nikon micro CT scanner (Derby, UK) with typical x-ray beam settings of 51kV and a 92 mA current, 1000 ms exposure time, two frames, and 3142 projections. Samples were mounted on a foam sample holder. No filtering was implemented, and the calculated scan resolution was 6.2 μm. The Nikon CT-Pro software was used to reconstruct the samples. VGSTUDIO MAX (Volume Graphics, Heidelberg, Germany) software was used to remove the foam, visualize, and measure the printed dosage forms.

2.4. FTIR-ATR spectroscopy

Samples were analysed with a Perkin Elmer Frontier FTIR-ATR spectrometer (Seer Green, UK) from 4000 cm^{-1} to 600 cm^{-1} with a scan resolution of 2 μm and step size of 0.5 cm^{-1}.

Three scans were collected for each sample. Prior to sample spectrum collection, a background was collected on the clean ATR crystal.

2.5. Raman spectroscopy

A LabRAM HR (Northhampton, UK) confocal Raman microscope equipped with a 784 nm infrared laser, 600 nm grating, 300 μm slit width, and 50x objective microscope lens was used to collect single point Raman spectra. Two accumulations were taken per scan with a 20s total acquisition time and spectra were analysed with the Horiba Scientific Jobin Yvon Lab Spec 6 Software.

2.6. Dissolution testing with HPLC characterization

Dissolution testing was performed using a Copely Scientific (Nottingham, UK) Tablet Dissolution Tester DIS 8000 according to USP specifications for carvedilol [USP, 2011] with rotating USP I baskets. The dissolution media was composed of 0.7 mL/L hydrochloric acid (HCl) diluted in ultra-pure water (σ=18.2 MΩ.cm, ELGA), adjusted to pH 1.5 with a 50 wt% NaOH aqueous solution. The test was performed at constant volume in 900 mL of dissolution media at 37°C. Throughout the dissolution test, five millilitre sample aliquots were removed at predetermined times and replaced with fresh media in order to maintain constant volume, then filtered with a 0.45 μm Millex PTFE hydrophilic filter (Millipore Ltd. Hertfordshire, UK).

Samples were characterized with an Agilent (Santa Clara, USA) HPLC Series 1100 system, equipped with an auto sampler, degasser and UV lamp. A wavelength of 240 nm was used to quantify the API. Method mobile phase compositions were 65% phosphate buffer and 35% acetonitrile (Fisher HPLC gradient grade). Phosphate buffer was composed of 2.72 g/L monobasic potassium phosphate (anhydrous, Sigma Aldrich) adjusted to pH 2.0 with

phosphoric acid (85-90%, Fluka). A Supelco (Sigma Aldrich) C18 Discovery column (5 μm, 25 cm x 4.6 mm diameter) was used to separate the samples at 35°C. A flowrate of 1.3 ml/min using a 20μL injection volume was implemented; runtime was 20 min. Carvedilol stock solutions were prepared according to the USP method [USP, 2014] by sonicating carvedilol (nominally 7 mg, Carbosynth) in 5 mL methanol (Fisher HPLC grade) and diluting the volume with dissolution media in a 250 mL volumetric flask. Standards were prepared with the stock solution and dissolution media. The standard calibration curve is included in the supplementary section, **Fig. A.1**. This HPLC method was also implemented to determine the initial carvedilol content in each printed geometry. Samples were leached separately in 250 mL dissolution media in volumetric flaks, sealed with Para film and magnetically stirred at room temperature. After two days, the samples were filtered (0.45 μm) and analysed for carvedilol content.

2.7. Ink fluid properties characterization

A Kruss GmbH (Hamburg, DE) Drop Shape Analyser DSA100 was used to evaluate the surface tension of the ink at ambient temperature with the Pendant Drop Method. The drop shape was analysed with the Kruss analysis software, with the Laplace-Young equation.

A Malvern (Malvern, UK) Kinexus rheometer fit with a cup and bob geometry was used to characterize the ink viscosity.

2.8. Dosage form leaching in ethyl acetate

Leaching of the printed geometries was carried out at room temperature in ethyl acetate (VWR, 99.9%). Samples were leached for two days in 20 mL ethyl acetate, with the media changed daily. After two days a final wash with 10 mL ethyl acetate was carried out for thirty

minutes. Samples were dried in a vacuum oven overnight at 50°C and stored in a vacuum desiccator.

2.9. HPLC characterization of carvedilol and NVP content in printed, leached samples

The carvedilol and NVP content of the leached samples was determined with the USP HPLC method. NVP standards and samples were prepared in acetonitrile (Fisher, HPLC gradient grade). Printed samples were leached separately in 50mL Para film sealed volumetric flasks for two days at room temperature with magnetic stirring. A calibration curve for NVP (**Fig. A.1)** and a carvedilol standard (110 ppm) were prepared. Samples and the standard(s) were analysed for carvedilol content with HPLC using an injection volume 5 μL. A 20 μL injection volume was implemented for NVP. Representative HPLC chromatograms of the samples and scans are included in the **supplementary** section, **Fig. A.3.**

2.10. Preparation of the printing ink

A drug containing ink solution with 0.50 wt% Irgacure 2959 (BASF), 10.00 wt% carvedilol (Carbosynth), 73.06 wt% NVP (Sigma Aldrich > 99%), 16.44 wt% PEGDA ($M_{n=}$ 250 g/mol, Sigma-Aldrich) was prepared by stirring the mixture at 25°C until dissolved. The mole ratio of NVP to PEGDA was fixed to 10:1. The curing behaviour of a series of NVP:PEGDA ink compositions was also determined by photocalorimetry and is included in **Table A.1 and Fig. A.4**. The ink was filtered using a 0.45 μm hydrophilic PTFE filter, sealed with a septum, degassed with N_2 (g), and loaded into a Dimatix 10pL print cartridge with a syringe. To prevent premature ink exposure to ambient light, cartridge loading was carried out in a dark room and the cartridge was wrapped several times in silver duct tape.

2.11. Ink printing parameters and BMP images

The carvedilol ink formulation was printed with a Dimatix DMP 2830 (Fujifilm Dimatix, Inc., Santa Clara, USA) printer equipped with a 365 nm (695 mW/cm^2, UV lamp, Printed Electronics PEL Tamworth, UK) lamp bolted to the print assembly and in line with the print path as previously described in [He et al., 2017] and [Clark et.al, 2017]. The printer was enclosed in a custom-built glove box and purged with N_2 (g), and oxygen levels were kept below 0.2%. The jetting firing voltage was 17-19.8V with a 3 kHz frequency and a drop speed adjusted to 1.00 mm in 130 s. All samples were printed at ambient temperature. Twenty non-jetting, UV post-curing layers were implemented for all print runs to further cure the dosage forms. Print specific parameters for each batch of dosage geometries such as the BMP digital image file used per layer, and the number of layers printed are tabulated in **Table 1**. The number of jets used ranged from 13 to 16, the maximum number of jets on the cartridge.

3. Results and Discussion

3.1. Ink characterization

The fluid flow properties of the ink were characterised and found to be suitable for printing. The operating ink viscosity and surface tension ranges for printing quoted by Dimatix are 2-12 centipose (cP) and 20-40 mN/m respectively [Fujifilm, 2008]. The measured ink viscosity was 4.50 +/- 0.01 cP (20°C, n=3) and the surface tension of the ink was 36.13 +/- 0.55 mN/m at ambient temperature (21.85°C, n=10), indicating the ink is within the recommended viscosity and surface tension ranges for the Dimatix printer.

3.2. Physical characterization of the printed dosage form geometries

Images of the printed geometries are included in **Figs. 1a, 1d , 1e** and the digital BMP files are illustrated in **Fig. 1c.** The printed geometries were robust (non-fragile), and easily handled. They appeared translucent and slightly yellow. In comparison, the formulated solutions were clear and slightly yellow, similar in appearance to the NVP liquid monomer. Optical microscopy (**Fig. 1a**) and the images indicate that the top surface of the tablets was topographically non-uniform; with bands corresponding to an individual print pass observed on the surface. In some cases, the deposition of excess ink (ring and thin film geometries, **Fig. 1d,e**) was also observed on the top surface, suggesting some leaking of the ink from the nozzle plate during printing. No evidence of crystallization within the dosage form (ijpr002) was observed in cross-polarized optical microscopy (**Fig. 1b**) or DSC. Melting peaks were not observed in the DSC thermogram of the solid dosage form, providing further evidence that carvedilol is an amorphous form within the printed polymeric matrix (**Fig. A.5**).

The thickness and diameter of the printed tablets are summarized in **Table 1,** as well as the digital image file dimensions. Tablet mass deviations were low, and no percent mass deviations exceeded USP specifications within each batch (10%, tablets <80 mg, USP 2000). Percent weight deviation for each tablet and all geometries is included in **Table A.2**. Tablet heights and diameters were also consistent. However, the dimensions of the tablets were observed to be larger than the image file specifications (up to 13%), as a result of the print resolution employed. The cause of these dimensional inconsistencies is unclear and may be attributed to ink spreading and variable ink curing speeds per batch. Free radical acrylate curing can be affected by the UV intensity or increased oxygen levels in the printing environment [Wight and Nunez, 1989]. The SA, V and SA/V ratio values for the dosages (**Table 2**) were calculated from the dimensional data in **Table 1**. The thin film geometries had the largest SA/V ratio, followed by the ring and cylindrical geometries.

An STL file (**Fig. A.6**) was then generated for each geometry from the digital bitmap image. The height of each geometry was estimated using the number of layers printed and the thickness per layer. The thickness per layer was determined from the measured height of the cylindrical tablets (ijpr002). It should be noted that the STL files represent only the intended dimensions, surface area, and volume of the printed geometries, and that the volume was kept constant. The SA, V and calculated SA/V ratios from the STL files are tabulated in **Table 2.**

3.3. FTIR-ATR characterization of the dosage forms

FTIR-ATR of the printed tablets (ijpr002, non-leached) suggests a high degree of curing in the dosage forms and the formation of a cross-linked network. The significant reduction in the PEGDA related acrylate double bond peaks (=CH_2 twist 810 cm^{-1}), and the NVP vinyl group (at 1629 cm^{-1}), suggest extensive Michael addition of the double bond and thus indication of the formation of a cross-linked polymer. A broad ester carbonyl peak from the cross-linked PEGDA is observed at 1729 cm^{-1}, and the peak at 1666 cm^{-1} is assigned to the amide C=O stretch of PVP. The assignment of the peak observed in the spectra at 1629 cm^{-1} is unresolved, as this can be attributed to the vinyl stretch of residual NVP and the aromatic C=C stretch of the drug. The characteristic aryl C=C stretches for carvedilol at 1608 cm^{-1} and 1591 cm^{-1} are observed in the tablets at 1607 cm^{-1} and 1589 cm^{-1}, respectively, indicating the incorporation of the drug into the dosage. Furthermore, a strong, broad peak at 3457 cm^{-1} indicates hydrogen bonded interactions in the cured dosage form.

For comparison, the FTIR spectrum of the drug-loaded ink is included in **Fig. 2a**. The characteristic C=C vinyl group stretch of NVP is observed at 1626 cm^{-1} and the peak observed at 1697 cm^{-1} is assigned to the C=O (amide) of NVP. A distinct characteristic C=O (ester) shift for the PEG acrylate functional group is not observed, and possibly is overlapped with the C=O (amide) NVP peak. The PEGDA acrylate =CH_2 (twist) is observed at 810 cm^{-1}

while, the characteristic saw-tooth shaped, secondary amine N-H stretch of carvedilol (3342 cm^{-1}) and the overlapping OH stretch are notably absent from the spectra, suggesting strong interactions between the carrier NVP-PEGDA ink and carvedilol. The broad (weak) peak at approx. 3392 cm^{-1} is attributed to hydrogen bonding [Lin-Vien et al., 1991].

3.4. Confocal Raman characterization of the dosage forms

Further characterization with Raman spectroscopy (**Fig. 2b**) confirmed the presence of carvedilol in the tablets. Assignments for the carvedilol were made in accordance with those reported by Marques et al., 2002. The carvedilol spectra exhibit a pyrrole ring breathing mode peak at 427.5 cm^{-1}, an N-H bend at 727.6 cm^{-1}, a C=C stretch/ring breathing peak at 1013.4 cm^{-1}, C=C stretching peaks at 1575.5 cm^{-1}, 1592.6 $cm^{-1}$and 1632.8 cm^{-1}, and characteristic peaks at 550.4 cm^{-1} and 1285.6 cm^{-1} (strong). The printed tablets exhibit API-related peaks at 423.7 cm^{-1}, 550.4 cm^{-1}, 726.1 cm^{-1}, 1014.8 cm^{-1}, 1285.6 cm^{-1}, 1576.2 cm^{-1}, 1590.7 cm^{-1} and 1628.4 cm^{-1}, further confirming the presence of carvedilol in the solid dosage form. Similar to the FTIR-ATR spectra of the tablet, the peak at 1628.4 cm^{-1} may be attributed to carvedilol (C=C stretching, aromatic) and unreacted NVP (C=C stretch) in the printed tablets. Finally, the drug-free cured ink exhibits characteristic peaks at 933.8 cm^{-1} and 1631.6 cm^{-1}, with the latter assigned to unreacted NVP.

3.5. Assay of the carvedilol content and residual monomer in the leached dosage forms

The materials palate for UV inkjet printing of pharmaceuticals is limited and persistence of residual unreacted material after UV curing is problematic, as residual unreacted monomer in the printed dosage forms is a concern due to possible toxicity [Norman et al., 2017]. The USP and FDA specify limits for unreacted NVP monomer in PVP based products with NVP content limited to 0.1 wt% in PVP copolymer (copovidone [USP, 2006a, b]) and cross-linked PVP (crospovidone) and 0.0001 wt% (10ppm) in pharmaceutical grade PVP (Povidone,

[USP, 2006c]). Furthermore, the FDA limits the amount residual monomer in PVP used in food additive applications to 1 wt% [FDA, 2017]. A post-processing leaching procedure was therefore implemented to remove unreacted monomer from the printed geometries. Ethyl acetate was selected to leach NVP from the printed dosages, as this solvent is miscible with NVP and PEGDA, exhibits low toxicity [FDA, 2017b], and can be readily removed. Cross-linked PEGDA and PVP are insoluble in ethyl acetate, and carvedilol exhibits low solubility in this solvent [Ha et al., 2019]. The final amount of unreacted NVP and recovered API for each printed geometry is summarized in **Table 3**. The dosage forms lost 5.4% to 10% of their original mass during leaching, and it should be noted that carvedilol, as well as NVP can be leached during this process (loss of carvedilol is between 2.3 wt% and 12.6 wt%). The residual NVP monomer concentrations in the leached ring, mesh and film geometries were shown to be within the USP limits for crospovidone and copovidone (0.1 wt%). The cylindrical tablets exhibited NVP content (0.18 wt%, by HPLC) above the USP limits for copovidone and crospovidone (0.1 wt%), but still within the FDA limit for PVP (1%) for food applications. Overall, drug loading in the dosage forms remains relatively high after leaching, and further experiments could be carried out to determine if lower residual NVP targets could be achieved on shorter timescales by implementing other solvents, or with longer leaching times in ethyl acetate.

3.6. Dissolution of the leached dosage forms

The USP and FDA guidance for carvedilol tablets and extended release carvedilol phosphate capsules specifies $HCl_{(aq)}$ dissolution medium [FDA, 2017c; USP, 2011] so as to promote sufficient drug solubility (via protonation) to allow analysis of released drug, and dissolution of the dosages was hence performed according to USP conditions for the printed carvedilol tablets.

There is an improvement in carvedilol solubility at lower pH because the drug ionizes, but it still meets the qualification for being an insoluble API (0.033 mg/ml in 0.1M HCl [Beattie et al., 2013] and 0.089 mg/ml in 0.1M HCl [Shah et al., 2011]). The dissolution profiles (**Fig. 3)** demonstrated over 80% carvedilol release, despite the relatively high loading (10 wt%) for all printed tablet geometries within ten hours, and complete release within twenty hours. The dosages were observed to swell during dissolution (and the assay) and did not remain intact (**Fig. A.2)**. Release was fastest for the thin films, followed by the ring and mesh geometries, and slowest for the cylindrical dosage forms. Faster release correlated to an increased surface area to volume ratio (SA/V) for the geometries (thin film > ring > cylinder) as calculated from the data in **Table 2**, showing that the formulation surface area is a controlling factor in release rate rather than any mechanism related to disintegration. This trend is in agreement with the literature [Lee et al., 2012; Goyanes et al., 2015; Martinez et al., 2018]. Similarly, the residual NVP content (**Table 3**), was lowest in the dosages with higher SA/V ratios, suggesting also that the leaching of the monomer may also be influenced by this ratio.

3.7. μCT imaging of the solid dosage forms

The surface area and volume of the cylindrical and mesh carvedilol dosages were characterized with μCT scanning imaging (**Table 4).** The μCT scans of the dosage forms are illustrated in **Fig. 4.** Pores were not observed in the μCT scans, suggesting the dosage forms are compact. **Table 4** indicates that the volume of the mesh dosage forms decreases after leaching by 8.81%. Given the density of NVP (1.04 g/mL), this volume decrease corresponds to an approximate mass loss of 9.16% and is comparable to the mass loss noted in **Table 2** for the mesh dosage forms. The volume of the cylindrical geometry measured with μCT is lower than that calculated based on manual measurement (**Table 2**) and similarly, the μCT measured surface area was larger than that calculated in **Table 2.** It should also be noted that

the resulting SA/V values for the cylindrical tablets calculated with the μCT imaging data are larger (by 213%) than those calculated in **Table 2**. These differences can be understood in terms of the volume shrinkage exhibited by photocurable materials during curing [Park et al., 2016] and an increased surface roughness resulting from the printing process.

4. Conclusions

Inkjet printing is a precise and scalable manufacturing method that can be used to produce pharmaceutical dosage forms. In this study, we demonstrate the feasibility of 3D inkjet printing a relatively highly drug-loaded (10 wt%) UV curable formulation for a poorly soluble API. The solid dosages were composed of carvedilol in a hydrophilic NVP and PEGDA cross-linked matrix. Several dosage geometries were printed and the release speed of carvedilol was characterized (thin films > ring, mesh>cylinder), thereby demonstrating different release profiles which can be accessed with a single ink. The weight variation of the printed solid dosages met USP specification. The release speed was demonstrated to increase with increased surface area to volume (SA/V) ratio for a cylindrical tablet to a mesh and ring geometry, to a thin film dosage form. The Raman and FTIR-ATR characterization of the tablets confirm the presence of an amorphous form of the drug in the tablets and suggest strong hydrogen bonding between the drug and the matrix. Finally, a post-processing leaching method to remove unreacted monomer in the printed dosage forms was investigated. Residual levels of monomer after leaching were demonstrated to be within the USP and FDA targets levels (0.1% for PVP related excipients copovidone and crospovidone) for several geometries (ring, film, mesh).

Acknowledgements

The work in this paper was funded by GlaxoSmithKline, Inc. Access to the Raman instrument was kindly provided by the Nottingham Nanoscale and Microscale Research Centre. Access to the Nikon μCT was kindly provided by Prof. R. Leach and imaging was carried out by Dr. H. Constantin and C. Fox. E. Clark thanks L. Korner, Dr. K. Datsiou, and

Dr. M. Simonelli for the μCT imaging analysis discussions and Dr. A. Aremu for the STL file discussion.

Appendix A. Supplementary data

The following is Supplementary data to this article:

A.1. Supplementary Information

Making Tablets for Delivery of Poorly Soluble Drugs Using Photoinitiated 3D inkjet printing

References

Lee et al., 2012 B. K. Lee, Y. H. Yun, J. S. Choi, Y.C., Jae Dong Kim and Y. W. Cho **Fabrication of drug-loaded polymer microparticles with arbitrary geometries using a piezoelectric inkjet printing system** Int. J. Pharm. 427 (2012), pp. 305-310 doi:10.1016/j.ijpharm.2012.02.011

Khaled et al., 2015 S.A. Khaled, J.C. Burley, M.R. Alexander, J.Yang and C.J. Roberts **3D printing of five-in-one dose combination polypill with defined immediate and sustained release profiles.** J. Control. Release 217 (2015), pp. 308-14 doi:10.1016/j.jconrel.2015.09.028.

Kyobula et al., 2017 M. Kyobula, A. Adedeji, M. R. Alexander, E. Saleh, R. Wildman, Ashcroft, P. R. Gellert and C. J. Roberts **3D inkjet printing of tablets exploiting bespoke complex geometries for controlled and tuneable drug release** J. Control. Release 261 (2017), pp. 207-15 doi: https://doi.org/10.1016/j.jconrel.2017.06.025

Genina et al., 2017 N. Genina, J. P. Boetker, S. Colombo, N. Harmankaya, J. Rantanen A. Bohr **Anti-tuberculosis drug combination for controlled oral delivery using 3D printed compartmental dosage forms: From drug product design to *in vivo* testing** J. Control. Release 268 (2017), pp. 40-48 doi: https://doi.org/10.1016/j.jconrel.2017.10.003

Rowe at al., 2000 C.W. Rowe, W.E. Katstra, R.D. Palazzolo, B.B. Giritlioglu, P. Teung, M.J. Cima Rowe **Multimechanism oral dosage forms fabricated by three dimensional printing™** J. Control. Release 66 (2000), pp. 11-17 doi: https://doi.org/10.1016/S0168-3659(99)00224-2

Goyanes et al., 2015 A. Goyanes, P. R. Martinez, A. Buanz, A.W. Basit, S. Gaisford **Effect of geometry on drug release from 3D printed tablets** Int. J. Pharm. 494 (2015), pp. 657-663 doi: https://doi.org/10.1016/j.ijpharm.2015.04.069

Goyanes et al., 2015b A. Goyanes, J. Wang, A. Buanz, R. Martínez-Pacheco, R. Telford, S. Gaisford and A.W. Basit **3D Printing of Medicines: Engineering Novel Oral Devices with Unique Design and Drug Release Characteristics** Mol. Pharmaceutics 12 (2015), pp. 4077–4084 doi: 10.1021/acs.molpharmaceut.5b00510

Solanki et al., 2018 N. G. Solanki, M. Tahsin, A.V. Shah, A.T.M. Serajuddin **Formulation of 3D Printed Tablet for Rapid Drug Release by Fused Deposition Modeling: Screening**

Polymers for Drug Release J. Pharm. Sci. 107 (2018) pp. 390-401doi: https://doi.org/10.1016/j.xphs.2017.10.021

Chai et al., 2017 X. Chai, H. Chai, X. Wang, J. Yang, J. Li, Y. Zhao, W. Cai, T. Tao and X. Xiang **Fused Deposition Modeling (FDM) 3D Printed Tablets for Intragastric Floating Delivery of Domperidone** Sci. Rep. 7 (2017), pp. 1-9 doi:https://doi.org/10.1038/s41598-017-03097-x

Clark et al., 2017 E.A. Clark, M.R. Alexander, D.J. Irvine, C.J. Roberts, M.J. Wallace, S. Sharpe, J. Yoo, Jae, R. J. M. Hague, C.J. Tuck and R.D. Wildman, Ricky D. (2017) **3D printing of tablets using inkjet with UV photoinitiation**. Int. J. Pharm. 529 (2017), pp. 523-530 doi: https://doi.org/10.1016/j.ijpharm.2017.06.085

Kalepu and Mekkanti, 2015 S. Kalepua and V. Nekkanti **Insoluble API delivery Insoluble drug delivery strategies: review of recent advances and business prospects** Acta Pharm. Sin. B 5 (2015), pp. 443-453 doi: https://doi.org/10.1016/j.apsb.2015.07.003

Bley et al., 2010 H. Bley, B. Fussnegger and R. Bodmeier **Characterization and stability of solid dispersions based on PEG/polymer blends** Int. J. Pharm. 390 (2010), pp. 165-173 doi: https://doi.org/10.1016/j.ijpharm.2010.01.039

Patterson et al., 2007 J. E. Patterson, M. B. James, A. H. Forster, R. W. Lancaster, J. M. Butler and T. Radesa **Preparation of glass solutions of three poorly water soluble drugs by spray drying, melt extrusion and ball milling** Int. J. Pharm. 336 (2007), pp. 22-34 doi: https://doi.org/10.1016/j.ijpharm.2006.11.030

Singh et al., 2017 G. Singh, l. Kaur, G. D. Gupta and S. Sharma **Enhancement of the Solubility of Poorly Water Soluble Drugs through Solid Dispersion: A Comprehensive Review** Indian J. Pharm. Sci. (2017), pp. 674-687 doi: 10.4172/pharmaceutical-sciences.1000279

Chokshi et al., 2017 R. J. Chokshi, N. H. Shah, H. K. Sandhu, A. W. Malick and H. Zia, **Stabilization of Low Glass Transition Temperature Indomethacin Formulations: Impact of Polymer-Type and Its Concentration** J. Pharm. Sci. 97 (2017), pp. 2286-2298 doi: 10.1002/jps.21174

Acosta-Vélez et al., 2017 G.F. Acosta-Vélez, C.S. Linsley, M.C. Craig, B. M. Wu **Photocurable Bioink for the Inkjet 3D Pharming of Hydrophilic Drugs** Bioengineering, 4 (2017), pp. 11 doi:10.3390/bioengineering4010011

Caló and Khutoryanskiy, 2015 Enrica Calo and Vitaliy V. Khutoryanskiy **Biomedical applications of hydrogels: A review of patents and commercial products**, Eur. Polym. J., 65 (2015), pp. 252-267 http://dx.doi.org/10.1016/j.eurpolymj.2014.11.024

Ergenc and Kizilel, 2011 T. I. Ergenc and S. Kizilel **Recent Advances in the Modeling of PEG Hydrogel Membranes for Biomedical Applications**, in: A. Laskovski (Ed.), Biomedical Engineering, Trends in Materials Science, InTech, Rijeka, 2011, pp. 307-346 doi:10.5772/12893

Fairbanks et al., 2009 B. D. Fairbanks, M. P. Schwartz, C. N. Bowman, K. S. Ansetha **Photoinitiated polymerization of PEG-diacrylate with lithium phenyl-2,4,6-trimethylbenzoylphosphinate: polymerization rate and cytocompatibility**, Biomaterials, 30 (2009), pp. 6702-6707 doi:10.1016/j.biomaterials.2009.08.055

FDA, 2017 US Food & Drug Administration, CFR - Code of Federal Regulations Title 21 21CFR173.55 Polyvinylpyrrolidone https://www.accessdata.fda.gov/scripts/cdrh/cfdocs/cfcfr/CFRSearch.cfm?fr=173.55 (accessed 19.10.17)

FDA, 2017b US Food & Drug Administration**, Q3C – Tables and List Guidance for Industry**. https://www.fda.gov/downloads/drugs/guidances/ucm073395.pdf (accessed 11.06.2018)

FDA, 2017c US Food & Drug Administration**, Dissolution Methods**. https://www.accessdata.fda.gov/scripts/cder/dissolution/dsp_getallData.cfm (accessed 08.08.2019)

Fujifilm, 2008 Fujifilm Dimatix, **Materials Printer & Cartridge DMP-2800 Series Printer & DMC-11600 Series Cartridge**. https://www.fujifilmusa.com/shared/bin/FAQs_DMP-2800_Series_Printer_DMC-11600+Series+Cartridge.pdf, 2008 (accessed 10.10.16)

GSK, 2017 GlaxoSmithKline, **Product Monograph COREG ® Carvedilol Tablets, HIGHLIGHTS OF PRESCRIBING INFORMATION** https://www.gsksource.com/coreg , 2017 (accessed 10.10.17)

Korsmeyer and Peppas, 1984 R.W. Korsmeyer and N. A. Peppas **Solute and penetrant diffusion in swellable polymers. III. Drug release from glassy poly (HEMA-co-NVP) copolymers**, J. Control. Release, 1 (1984), pp. 89-98 doi: 10.1016/0168-3659(84)90001-4

Lago et al., 2015 M. A. Lago, A. Rodríguez-Bernaldo de Quirós, R. Sendón, J. Bustos, M. T. Nieto, P. Paseiro **Photoinitiators: a food safety review**, Food Addit. Contam. A, 32 (2015), pp. 779-798 doi: 10.1080/19440049.2015.1014866

Lee et al., 2014 C-Y. Lee, F. Teymour, H. Camastral, N. Tirelli, J. A. Hubbel, D. L. Elbert, G. Papavasiliou **Characterization of the Network Structure of PEG Diacrylate Hydrogels Formed in the Presence of N-Vinyl Pyrrolidone**, Macrolmol. React. Eng., 8 (2014), pp. 314-328 doi: 10.1002/mren.201300166

Marques et al., 2002 M.P.M Marques, P. J. Oliveira, A. J. M. Moreno, L. A. E. Batista de Carvalho **Study of carvedilol by combined Raman spectroscopy and ab initio MO calculations** J. Raman Spectrosc., 33 (2002), pp.778-783 doi: 10.1002/jrs.916

Maximilien, 2009 J. S. Maximilien **Polyethylene Oxide**, in: R. C. Rowe, P.J. Sheskey, M. E. Quinn (Eds.), Handbook of Pharmaceutical Excipients, Sixth ed., Pharmaceutical Press, London, 2009, pp. 522-524

Norman et al., 2017 J. Norman, R.D. Madurawe, C.M.V. Moore, M. A. Khan, A. Khairuzzaman **A new chapter in pharmaceutical manufacturing: 3D-printed drug products** Adv. Drug Deliv. Rev., 108 (2017), pp. 39-50 doi: 10.1016/j.addr.2016.03.001

Nguyen et al., 2013 A. K. Nguyen, S. D. Gittard, A. Koroleva, S. Schlie, A. Gaidukeviciute, B. N. Chichkov, R. J. Narayan **Two-photon polymerization of polyethylene glycol diacrylate scaffolds with riboflavin and triethanolamine used as a water-soluble photoinitiator**, Regen. Med., 8 (2013), pp. 725-738 doi: 10.2217/rme.13.60

Riger and Peppas, 1987 P.L. Ritger, N.A. Peppas **A simple equation for description of solute release I. Fickian and non-fickian release from non-swellable devices in the form of slabs, spheres, cylinders or discs** J. of Control. Release, 5 (1987), pp. 23-36 doi: 10.1016/0168-3659(87)90034-4

USP, 2000 United States Pharmacopeia and National Formulary (USP 24- NF 19), The United States Pharmacopeial Convention, Rockville, MD, USA 2000 <905> Uniformity of Dosage Forms https://www.usp.org/sites/default/files/usp/document/harmonization/gen-method/q0304_pf_30_4_2004.pdf

USP, 2006a United States Pharmacopeia and National Formulary (USP 29-NF 24), The United States Pharmacopeial Convention, Rockville, MD, USA pp. 3316-3317

USP, 2006b United States Pharmacopeia and National Formulary (USP 29-NF 24), The United States Pharmacopeial Convention, Rockville, MD, USA pp. 3320-3321

USP, 2006c United States Pharmacopeia and National Formulary (USP 29-NF 24), The United States Pharmacopeial Convention, Rockville, MD, USA pp. 1777-3321

USP, 2011 United States Pharmacopeia and National Formulary (USP 36- NF 31), The United States Pharmacopeial Convention, Rockville, MD, USA, 2011 pp. 4621

Vehse et al., 2014 M. Vehse, S. Petersen, K. Sternberg, K.-P. Schmiz, H. Seiz**Drug delivery from poly(ethylene glycol) diacrylate scaffolds produced by DLC based micro-Stereolithography** Macromol. Symp., 346 (2014), pp. 43-47, 10.1002/masy.201400060

Wang et al., 2016 J. Wang, A. Goyanes, S. Gaisford, A.W. Basit **Stereolithographic (SLA) 3D printing of oral modified-release dosage forms** Int. J. Pharm., 503 (2016), pp. 207-212, 10.1016/j.ijpharm.2016.03.016

Dhariwala et al., 2004 B. Dhariwala, E. Hunt and T. Boland **Rapid prototyping of tissue-engineering constructs, using photopolymerizable hydrogels and stereolithography** Tissue Eng. 10 (2004), pp. 1316–1322 doi: 10.1089/ten.2004.10.1316

Chan et al., 2010 V. Chan, P. Zorlutuna, J.H. Jeong, H. Kong, R. Bashir **Three-dimensional photopatterning of hydrogels using stereolithography for long-term cell encapsulation** Lab on a Chip 10 (2010), pp. 2062–2070 doi: 10.1039/c004285d

Seck at al. 2010 T.M. Seck, F.P.W. Melchels, J. Feijen and D.W. Grijpma **Designed biodegradable hydrogel structures prepared by stereolithography using poly(ethylene glycol)/poly(D,L-lactide)-based resins** J. Control. Release 148 (2010), pp. 34–41 doi:10.1016/j.jconrel.2010.07.111

Gu et al., 2016 B. K. Gu, D. J. Choi, S.J. Park, M.S. Kim, C. M. Kang and C-H. Kim **3-dimensional bioprinting for tissue engineering applications** Biomaterials Research 20 (2016), pp. 1-8 doi:10.1186/s40824-016-0058-2

Jansen et al., 2003 J. F. G. A. Jansen, A. A. Dias, M. Dorschu, and B. Coussens **Fast Monomers: Factors Affecting the Inherent Reactivity of Acrylate Monomers in Photoinitiated Acrylate Polymerization** Macromolecules 36 (2003) pp. 3861-3873 doi:10.1021/ma021785r

Ligon et al., 2017 S. C. Ligon, R. Liska, J. Stampfl, M. Gurr and R. Mülhaupt **Polymer for 3D Printing and Customized Additive Manufacturing** Chem. Rev. 117 (2017), pp. 10212−10290 doi: 10.1021/acs.chemrev.7b00074

Guvendiren et al., 2016 M. Guvendiren, J. Molde, R.M.D. Soares and J. Kohn **Designing Biomaterials for 3D orienting** ACS Biomater. Sci. Eng. 10 (2016) pp. 1679-1693 doi:10.1021/acsbiomaterials.6b00121

Jansen et al., 2009 J. Jansen, F.P.W. Melchels, D. W. Grijpma, J. Feijen **Fumaric Acid Monoethyl Ester-Functionalized Poly(D,L-lactide)/N-vinyl-2-pyrrolidone Resins for the Preparation of Tissue Engineering Scaffolds by Stereolithography** Biomacromolecules. 10 (2009), pp. 214–220 doi:10.1021/bm801001r

Gao et al., 2015 G. Gao, A.F. Schilling, K. Hubbell, T. Yonezawa, D. Truong, Y. Hong, G. Dai, X. Cui **Improved properties of bone and cartilage tissue from 3D inkjet-bioprinted human mesenchymal stem cells by simultaneous deposition and photocrosslinking in PEG-GelMA** Biotechnol. Lett. 11 (2015) pp. 2349–2355 doi: 10.1007/s10529-015-1921-2

Knopp et al., 2015 M. M. Knopp, L. Tajber, Y. Tian, N. E. Olesen, D. S. Jones, A. Kozyra, K. Löbmann, K. Paluch, C. M. Brennan, R. Holm, A. M. Healy, G. P. Andrews, and T. Rades **Comparative Study of Different Methods for the Prediction of Drug–Polymer Solubility** Mol. Pharmaceutics 12 (2015), pp. 3408-3419 doi:10.1021/acs.molpharmaceut.5b00423

Hacker et al., 2009 M.C. Hacker, A. Haesslein, H. Ueda, W.J. Foster, C.A. Garcia, D.M. Ammon, R.N. Borazjani, J.F. Kunzler, J.C. Salamone, A.G. Mikos **Biodegradable fumarate-based drug-delivery systems for ophthalmic applications** J. Biomed. Mater. Res. A 88 (2009), pp. 976-989 doi: 10.1002/jbm.a.31942

White et al., 2006 T. J. White, W. B. Liechty, C. A. Guymon **Copolymerization of N-Vinyl Pyrrolidinone with Multifunctional Acrylates** RadTech Technical Proceedings 2006 http://www.radtechmembers.org/archive-proceedings/2006/papers/068.pdf (accessed 12.06.2018)

Perkin Elmer, 2014 Perkin Elmer **UV/DSC Study on New Double Furnace DSC** http://www.perkinelmer.co.uk/lab-solutions/resources/docs/PRD_UV_DSC_Study_on_New_Double_Furnace_011616_01.pdf (accessed 12.06.2018)

Peng et al., 2014 H. Penga, M. Nia, S. Bia, Y. Liaoa and X. Xie **Highly diffractive, reversibly fast responsive gratings formulated through holography** RSC Adv., 4 (2014), pp. 4420-4426 doi:10.1039/C3RA45570J

Hwang et al., 2011 H-D. Hwang, C-H. Park, J-I Moon, H-J. Kim, T. Masubuchi **UV-curing behavior and physical properties of waterborne UV-curable polycarbonate-based polyurethane dispersion** Prog. Org. Coat. 72 (2011), pp. 663-675 doi:http://www.sciencedirect.com/science/article/pii/S030094401100227X

Martinez et al., 2018 P.R. Martinez, A. Goyanes, A.W. Basit, A.W. et al. **Influence of Geometry on the Drug Release Profiles of Stereolithographic (SLA) 3D-Printed Tablets** AAPS PharmSciTech (2018), pp. 1-7 https://doi.org/10.1208/s12249-018-1075-3

Do et al., 2018 A-V. Do, K. S. Worthington, B. A. Tucker, A. K. Salem **Controlled drug delivery from 3D printed two-photon polymerized poly(ethylene glycol) dimethacrylate devices** Int. J. Pharm. 552 (2018), pp. 217-224 https://doi.org/10.1016/j.ijpharm.2018.09.065

Yang et al., 2018 Y. Yang, H. Wang, H. Li, Z. Ou, G.Yang, **3D printed tablets with internal scaffold structure using ethyl cellulose to achieve sustained ibuprofen release** Eur. J. Pharm. Sci., 115 (2018), pp. 11–18 doi: https://doi.org/10.1016/j.ejps.2018.01.005

Martinez et al., 2017 P. R. Martinez, A. Goyanes, A.W. Basit, S. Gaisford **Fabrication of drug-loaded hydrogels with stereolithographic 3D printing** Int. J. Pharm. 532 (2017), pp. 313–31 doi: http://dx.doi.org/10.1016/j.ijpharm.2017.09.003

Okwuosa et al., 2018 T.C. Okwuosa, C. Soares, V. Gollwitzer, R. Habashy, P. Timmins, M.A. Alhnan **On demand manufacturing of patient-specific liquid capsules via co-ordinated 3D printing and liquid dispensing** Eur. J. Pharm. Sci. 118 (2018), pp. 134-143 doi:10.1016/j.ejps.2018.03.010

Yuvaraja and Khanam, 2014 K. Yuvaraja, J. Khanam **Enhancement of carvedilol solubility by solid dispersion technique using cyclodextrins, water soluble polymers and hydroxyl acid** J. Pharm. Biomed. Anal. 96 (2014), pp. 10-20 doi: 10.1016/j.jpba.2014.03.019

Louzao et al., 2018 I. Louzao, B. Koch, V. Taresco, L. Ruiz-Cantu, D. J. Irvine, C. J. Roberts, C. Tuck, C. Alexander, R. Hague, R. Wildman, and M. R. Alexander **Identification of Novel "Inks" for 3D Printing Using High-Throughput Screening: Bioresorbable Photocurable Polymers for Controlled Drug Delivery** ACS Appl. Mater. Interfaces 10 (2018), pp. 6841–6848 doi:10.1021/acsami.7b15677

Park et al., 2016 J-W. Park, G-S. Shim, J-H. Back, H-J. Kim, S. Shin, T-S. Hwang **Characteristic shrinkage evaluation of photocurable materials** Polymer Testing 56 (2016), pp. 344-353 doi: https://doi.org/10.1016/j.polymertesting.2016.10.018

Ha et al., 2019 E.-S.Ha, J.-S. Kim, S-K. Lee, W.-Y. Sima, J.-S. Jeong, M.-S. Kim **Equilibrium solubility and solute-solvent interactions of carvedilol (Form I) in twelve mono solvents and its application for supercritical antisolvent precipitation** J. Mol. Liq 294 (2019), pp.1-7 doi: https://doi.org/10.1016/j.molliq.2019.111622

Beattie et al., 2013 K. Beattie, G. Phadke, J. Novakovic **Carvedilol**, in: H.G Brittain (Ed.), Profiles of Drug Substances, Excipients and Related Methodology 38, Academic Press, San Diego, 2013, pp. 113-157 doi: 10.1016/B978-0-12-407691-4.00004-6

Prado et al., 2014 L. D. Prado, H. V. A. Rocha, J. A. L. C. Resende, G. B. Ferreira, A. M. R. de F. Teixeira, **An insight into carvedilol solid forms: effect of supramolecular interactions on the dissolution profiles** Cryst. Eng. Comm., 16 (2014), pp. 3168-3179 doi: 10.1039/c3ce42403k

Shah et al., 2011 R. Shah, S. Patel, H. Patel, S. Pandey, S. Shah, D. Shah **Development and validation of dissolution method for carvedilol compression-coated tablets** Braz. J. Pharm. Sci. 47 (2011), pp. 899-906
doi: http://dx.doi.org/10.1590/S1984-82502011000400027

Menon et al., 2012 S.K. Menon, B. R. Mistry, K. V. Joshi, N. R. Modi, D. Shashtri **Evaluation and solubility improvement of carvedilol: PSC[n]arene inclusion complexes with acute oral toxicity studies** J. Incl. Phenom. Macrocycl. Chem. 73 (2012), pp. 295–303doi: https://doi.org/10.1007/s10847-011-0056-x

Table(1)

Table 1: Dimensions, print parameters and masses for each batch of dosage forms.

	Cylinder ijpr002* **	**Cylinder ijpr010**** **	**Thin Film**** **	**Ring**	**Mesh **** **
BMP Geometry	circle	circle	square	ring	mesh
BMP dimensions (mm)	7.02	7.02	11.01 x 11.01	8.49	8.52
Print dimensions (mm)	7.04 ± 0.01	7.75 ± 0.03*	12.51 ± 0.05 x 12.45 ± 0.04	9.27 ± 0.02 x 9.45 ± 0.03 (n=7)**	9.31 ± 0.04 x 9.14 ± 0.04
Deviation of print from BMP file (%)	0.2279 ± 0.13	10.4 4± 0.41	13.08 ± 0.58 - 13.61 ± 0.41	10.27 ± 0.25 (n=7)	7.22 ± 0.51
Print height (mm)	1.62 ± 0.01	1.41 ± 0.03*	0.56 ± 0.03	1.53 ± 0.03 (n=7)	1.54 ± 0.04
No. layers printed	200	200	64	188	160
Cartridge height (mm)	1	2	1	1	1
No. jets used	16	16	16	13	15
Mass (mg)	50.97 ± 0.15	50.68 ± 0.35 (n=13)	53.87 ± 0.44 (n=12)	50.80 ± 0.14 (n=9)	59.61 ± 0.51 (n=12)

* measured after leaching in ethyl acetate

** Case wall thickness: 2.34+/- 0.01 (n=2). Case wall thickness of BMP image file was 2.00mm.

*** n=15 for all measurements

*** *n=10 for all measurements unless specified

Table(2)

Table 2: Surface area (SA), volume (V) and SA/V ratio for each batch of dosage forms and the STL files

	Cylinder ijpr002* **	**Cylinder ijpr010**** **	**Thin Film**** **	**Ring**	**Mesh **** **
Print volume, V (mm^3)	62.94 ± 0.46	66.57 ± 1.57	87.20 ± 3.47	79.50 ± 0.21	-
Print Surface area, SA (mm^2)	113.5 ± 0.4	128.8 ± 1.0	339.4 ± 2.4	171.05 ± 0.29 (n=2)	-
Print SA/V ratio (mm^{-1})	1.804 ± 0.009	1.934 ± 0.034	3.897 ± 0.146	2.151 ± 0.009 (n=2)	-
Height of STL (mm)	1.62	1.62	0.518	1.523	1.296
Calculated V from STL (mm^3)	62.693	62.693	62.768	60.277	62.596
Calculated SA from STL (mm^2)	113.127	113.127	265.244	141.783	176.719
Calculated SA/V ratio from STL (mm^{-1})	1.8	1.8	4.23	2.35	2.82

* measured after leaching in ethyl acetate

** Case wall thickness: 2.34+/- 0.01 (n=2). Case wall thickness of BMP image file was 2.00mm.

*** n=15 for all measurements

*** *n=10 for all measurements unless specified

Table(3)

Table 3: HPLC measurement results for the leached printed tablets

	cylinder (ijpr010)* **	**ring (ijpr003)**	**mesh (ijpr005)**	**thin film (ijpr009)**
Carvedilol dose per dosage form (mg)	4.68 ± 0.10	4.63 ± 0.05	5.44 ± 0.06	4.44 ± 0.04
Percent carvedilol loading (%)*	10.3 ± 0.1	9.65 ± 0.06	9.85 ± 0.04	9.16 ± 0.04
NVP monomer detected by HPLC (mg)	0.076 ± 0.015	0.025 ± 0.001	0.017 ± 0.001	0.011 ± 0.002
Percent NVP in dosage form (wt%) **	0.178 ± 0.037	0.057 ± 0.001	0.035 ± 0.002	0.026 ± 0.005
Total mass loss after drying and leaching (%)	5.92 ± 0.26	5.41 ± 0.32	7.29 ± 0.05	9.95 ± 0.58
Carvedilol detected in **non-leached** printed dosage (mg)	4.79 ± 0.06	5.18 ± 0.01	5.98 ± 0.02	5.08 ± 0.04

*Calculation based on carvedilol detected and the dried, final leached mass

** Calculated with (mass NVP detected) / (final leached mass - amount of API detected) x 100

*** Solid dosages dried overnight at 50°C **prior** to solvent leaching. Carvedilol detected in non-leached cylinders (ijpr002) was 5.12 ± 0.17 mg

Table(4)

Table 4: Tabulated CT scan surface area (SA) and volume (V) results for the printed dosages.

	Volume, V (mm^3)	**Surface area, SA (mm^2)**	**SA/V (mm^{-1})**
Cylinder 11, leached (ijpr010)	38.9	160.37	4.12
Mesh 5, leached (ijpr005)	44.5	278.61	6.26
Mesh 14, non-leached (ijpr005)	48.8	267.48	5.48

Captions

Fig. 1. Images of the printed geometries. **a)** Optical microscopy (reflection) and **b)** cross polarized optical microscopy (transmission) of a cylindrical tablet **c)** BMP 2D images used to build the 3D geometries **d)** images of dosages printed (top scale in mm) **e)** images of the tablets after leaching and drying. The scale is in mm.

Fig. 2. Spectroscopic characterization of the starting materials and dosage forms. **a)** FTIR-ATR for the printed cylindrical tablets (n=10 scans), PEGDA, NVP, the carvedilol loaded ink formulation, and carvedilol **b)** confocal Raman microscopy of a leached cylindrical tablet (blue), a cylindrical tablet (black), a drug free (API-free) tablet (grey) and carvedilol (red).

Fig. 3. Release behaviour of carvedilol from the printed dosage forms in USP (pH 1.5) HCl dissolution media. Error bars indicate standard deviation. n=4 for cylindrical geometries and n=3 for thin film, mesh and ring geometries.

Fig. 4. μCT Images of the dosage forms. **a)** A leached cylindrical tablet (ijpr010) **b)** a leached mesh tablet **c)** a non-leached mesh tablet.

Figure(1)

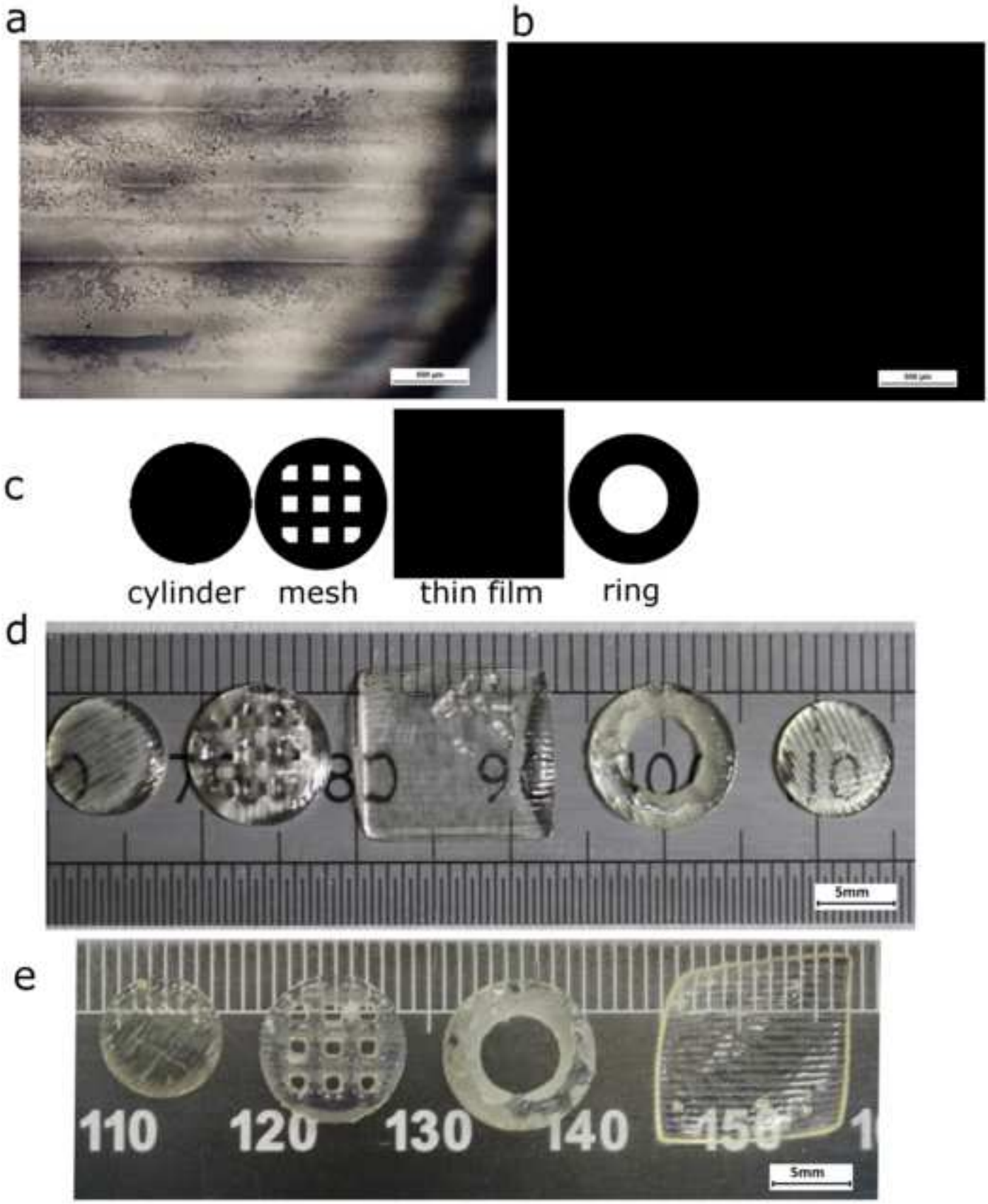

Figure(2)

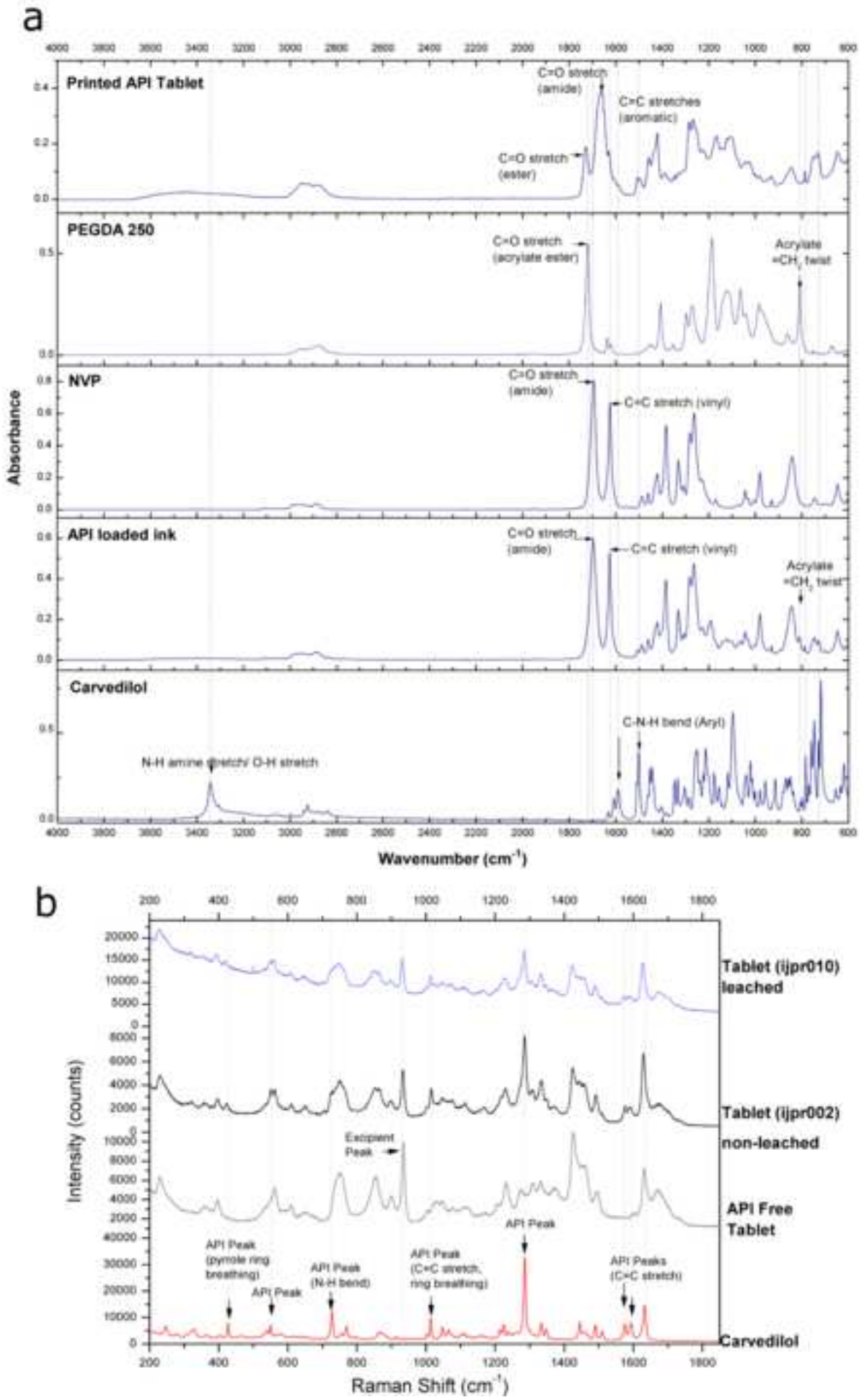
a
Printed API Tablet
C=O stretch (amide)
C=C stretches (aromatic)
C=O stretch (ester)
PEGDA 250
C=O stretch (acrylate ester)
Acrylate =CH2 twist
NVP
C=O stretch (amide)
C=C stretch (vinyl)
API loaded ink
C=O stretch (amide)
C=C stretch (vinyl)
Acrylate =CH2 twist
Carvedilol
C-N-H bend (Aryl)
N-H amine stretch/ O-H stretch
Absorbance
Wavenumber (cm-1)
b
Tablet (ijpr010) leached
Tablet (ijpr002) non-leached
Excipient Peak
API Free Tablet
API Peak
API Peak (pyrrole ring breathing)
API Peak
API Peak (N-H bend)
API Peak (C=C stretch, ring breathing)
API Peaks (C=C stretch)
Carvedilol
Intensity (counts)
Raman Shift (cm-1)

Figure(3)

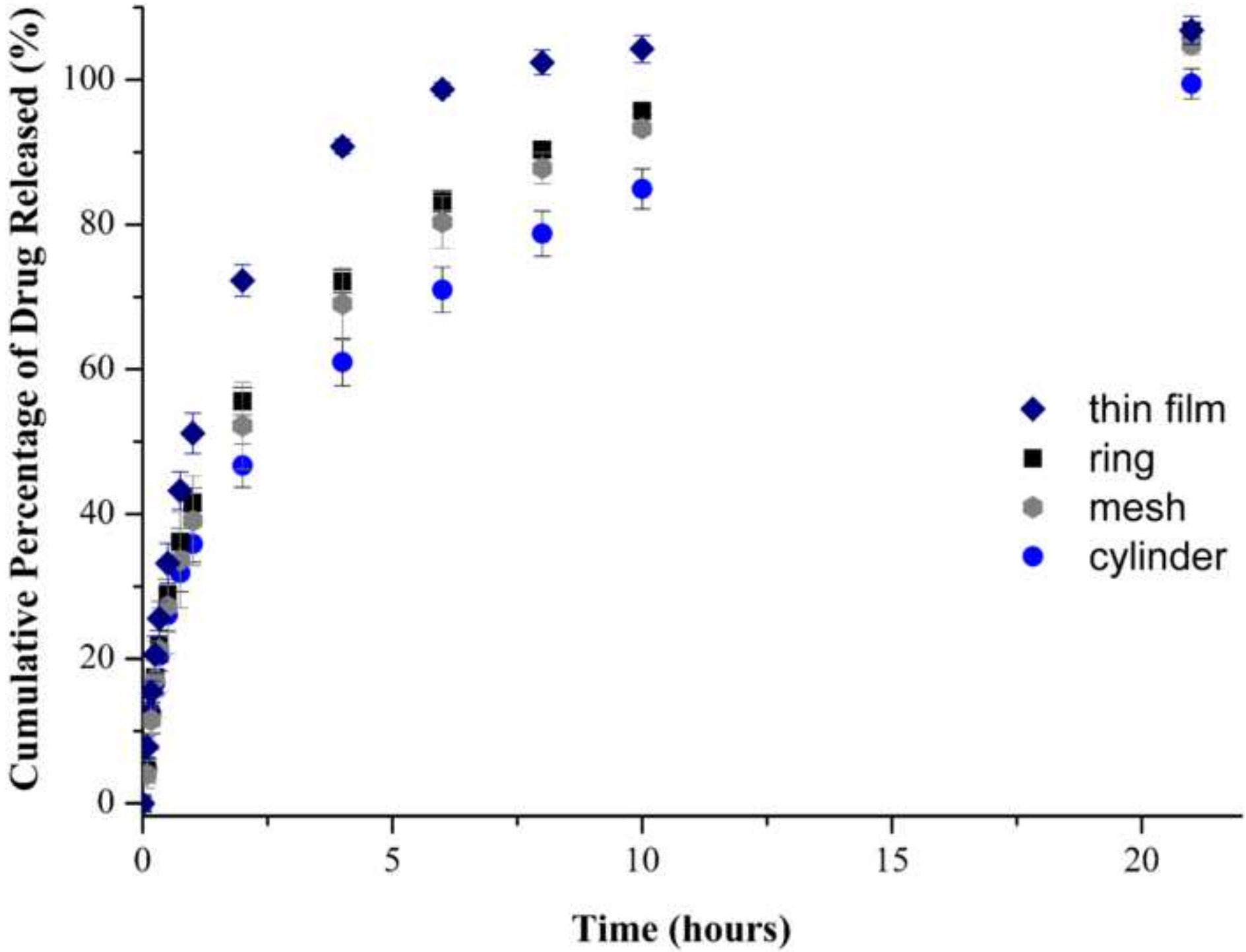
Cumulative Percentage of Drug Released (%)
0
20
40
60
80
100
0
5
10
15
20
Time (hours)
thin film
ring
mesh
cylinder

Figure(4)

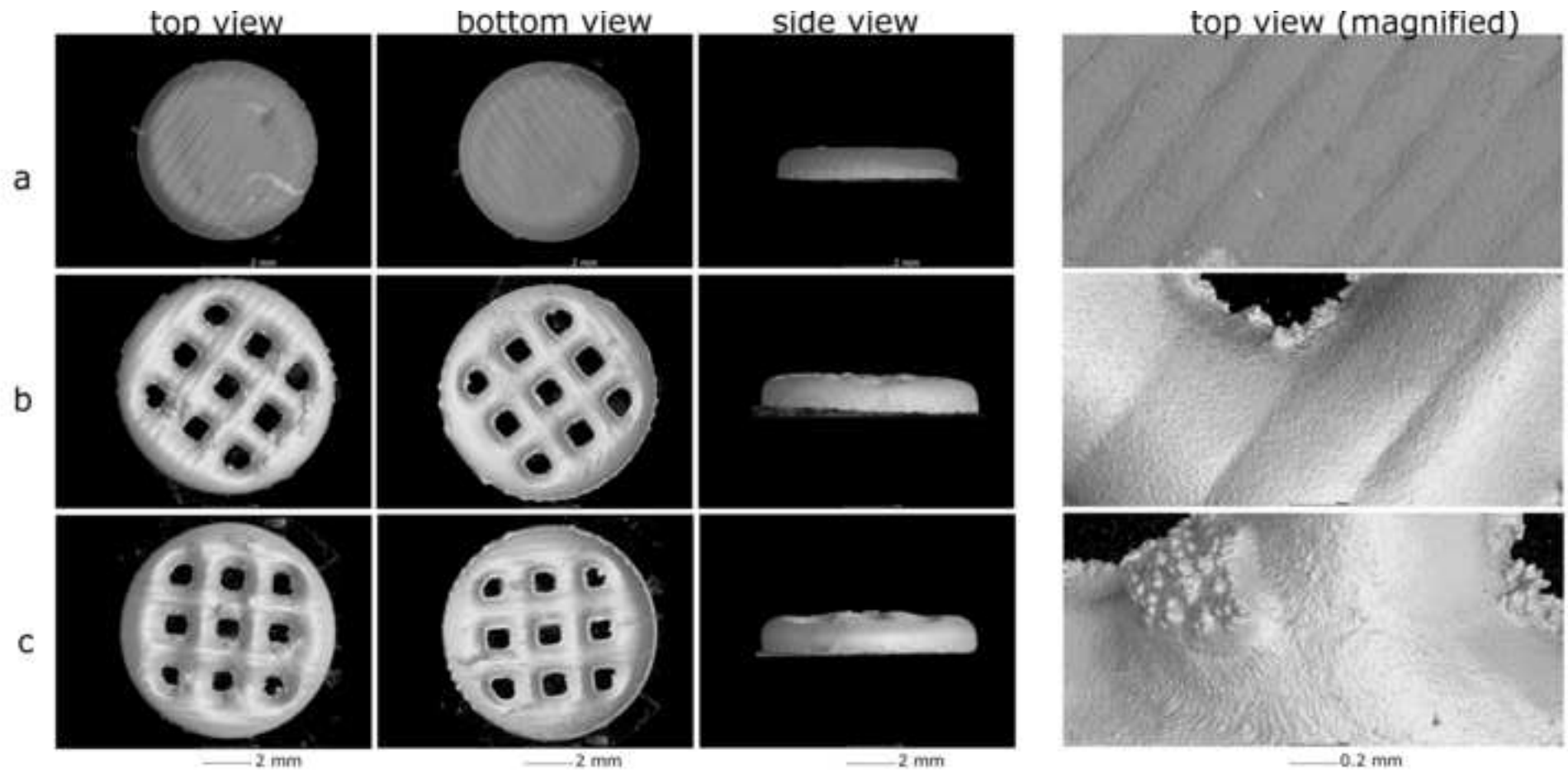
top view
bottom view
side view
top view (magnified)
a
b
c
2 mm
2 mm
2 mm
0.2 mm

Supplementary Material

Click here to download Supplementary Material: A. Appendix Supplementary Data.docx